Journal of Physics: Conference Series **321** (2011) 012022 doi:10.1088/1742-6596/321/1/012022

Covariant Density Functional Theory for Excited States in Nuclei.

Ioannis Daoutidis[1], Elena Litvinova[2,3], and Peter Ring[4]

[1] Institut d'Astronomie et d'Astrophysique, Université Libre de Bruxelles, B-1050, Belgium
[2] GSI Helmholtzzentrum für Schwerionenforschung, 64291 Darmstadt, Germany
[3] Institut für Theoretische Physik, Goethe-Universität, 60438 Frankfurt am Main, Germany
[4] Physik-Department der Technischen Universität München, D-85748 Garching, Germany

E-mail: idaoutid@ulb.ac.be,e.litvinova@gsi.de,ring@ph.tum.de

Abstract. Recent applications of covariant density functional theory (CDFT) for the description of excited states in nuclei are discussed. They are based on the Runge-Gross theorem of time-dependent density functional theory. In the adiabatic approximation, where the energy dependence of the self-energy is neglected one obtains in the small amplitude limit RPA and QRPA. In order to describe the width of giant resonances an energy dependent self energy is constructed by coupling to surface modes of the system. Recent applications with $2qp$-phonon and 2-phonon configurations are discussed.

1. Introduction

Since one of the underlying symmetries of QCD is Lorentz invariance covariant density functional theory [1, 2] is of particular interest in nuclear physics. This symmetry not only allows to describe in a consistent way the spin-orbit coupling which has an essential influence on the underlying shell structure, but it also puts stringent restrictions on the number of parameters in the corresponding functionals without reducing the quality of the agreement with experimental data. Density functional theory originally introduced by Kohn and Sham [3] in the sixties is based on the mean field concept and strictly valid only for a description of the ground states. In fact density functionals presently in use are adjusted to ground state properties. It is therefore an interesting question, to what extend those functionals can be used also for the description of excited states in nuclear physics.

2. Time dependent density functional theory.

In Coulombic system density functional theory has been extended over the years also for excited states in the framework of time-dependent density functional theory (TDDFT) [4]. Runge and Gross could derive a theorem [5] which is an extension of the Kohn-Sham method. They consider a many-body problem in a time-dependent external single potential $f_{ext}(\mathbf{r},t)$ with the exact solution $|\Psi(t)\rangle$ for a given initial condition $|\Psi(0)\rangle$. They could show that for given initial conditions there is a one-to-one correspondence between the exact time-dependent local single particle density $\rho(\mathbf{r},t)$ and the external potential $f_{ext}(\mathbf{r},t)$. As in static Kohn-Sham theory there exists a fictitious system of non-interacting particles with the single particle wave functions

$\phi_i(\mathbf{r},t)$ $(i = 1 \dots N)$ that satisfy time-dependent Kohn-Sham equations of the form

$$i\partial_t \phi_i(\mathbf{r},t) = \left[-\nabla^2/2m + v[\rho](\mathbf{r},t)\right] \phi_i(\mathbf{r},t). \tag{1}$$

where $\rho(\mathbf{r},t) = \sum_i^N |\phi_i(\mathbf{r},t)|^2$ is the exact local density. The time-dependent Kohn-Sham potential $v[\rho](\mathbf{r},t)$ is a function of $\mathbf{r}$ and t, but it is in addition a unique functional of the time-dependent density $\rho(\mathbf{r},t)$. The situation looks similar to static Kohn Sham theory but it is much more complicated. The mean field potential $v[\rho](\mathbf{r},t)$ contains the entire history of the system and its derivation would require the full solution of the exact Schrödinger equation for arbitrary systems with the density $\rho(\mathbf{r},t)$.

However, if the external potential $f_{ext}(\mathbf{r},t)$ is weak, the situation can be simplified considerably and linear response theory is applicable. This case applies also to nuclear physics. We do not need to know the functional $v[\rho](\mathbf{r},t)$ for arbitrarily changing densities, rather we need it only in the vicinity of the initial density, e.g. of the static ground state density $\rho_s(\mathbf{r})$ of the system and we can write $\rho(t) = \rho_s + \delta\rho(t)$. Going up to linear order in f_{ext}, we obtain

$$v[\rho_s + \delta\rho](\mathbf{r},t) = v_s[\rho_s](\mathbf{r}) + \int dt' \int d^3r' V[\rho_s](\mathbf{r},t,\mathbf{r}',t')\delta\rho(\mathbf{r}',t'). \tag{2}$$

Here V is an effective interaction, the derivative of the mean field with respect to the density

$$V(\mathbf{r},\mathbf{r}',t-t') = \left.\frac{\delta v(\mathbf{r},t)}{\delta\rho(\mathbf{r}',t')}\right|_{\rho=\rho_s}. \tag{3}$$

It is a functional of the static density ρ_s and for a time independent Hamiltonian it depends only on the time difference $t - t'$ [4]. Introducing as usual the response function $R(\mathbf{r},t,\mathbf{r}',t')$

$$\delta\rho(\mathbf{r},t) = \int d^3r' \int dt' R(\mathbf{r},\mathbf{r}',t-t') f_{ext}(\mathbf{r}',t') \tag{4}$$

we find after a Fourier transformation in time the well known linear response equation [6]

$$R(\mathbf{r},\mathbf{r}',\omega) = R_0(\mathbf{r},\mathbf{r}',\omega) + \int d^3r_1 \int d^3r_2 R_0(\mathbf{r},\mathbf{r}_1,\omega) V(\mathbf{r}_1,\mathbf{r}_2,\omega) R(\mathbf{r}_2,\mathbf{r}',\omega) \tag{5}$$

Of course, all these quantities are functionals of the exact ground state density $\rho_s(\mathbf{r})$. For a weak external field f_{ext}, these equations are exact, but, of course, we do not know the functional $v[\rho](\mathbf{r},t)$ in Eq. (1) nor its functional derivative at $\rho = \rho_s$. As usual in density functional theory the Runge-Gross theorem gives us no hint, how to derive these quantities. We therefore need some model for this single particle potential $v[\rho](\mathbf{r},t)$ in the Kohn-Sham equation.

3. The adiabatic approximation

There is a very common approximation, the so called *adiabatic approximation*. Here one neglects the memory and assumes that the density changes only very slowly, such that the potential is given at each time by the static potential v_s corresponding to this density.

$$v[\rho](\mathbf{r},t) \approx v_s[\rho_s](\mathbf{r},t) \tag{6}$$

In this approximation $v[\rho]$ is no longer depending on the function $\rho(\mathbf{r},t)$ of 4 variables, but rather on the function $\rho_s(\mathbf{r}) = \rho(\mathbf{r},t)$ depending only on three variables at a given time. t is here only a parameter. The effective interaction is the second derivative of the static energy functional with respect to the static density at a given time t. In Fourier space this interaction

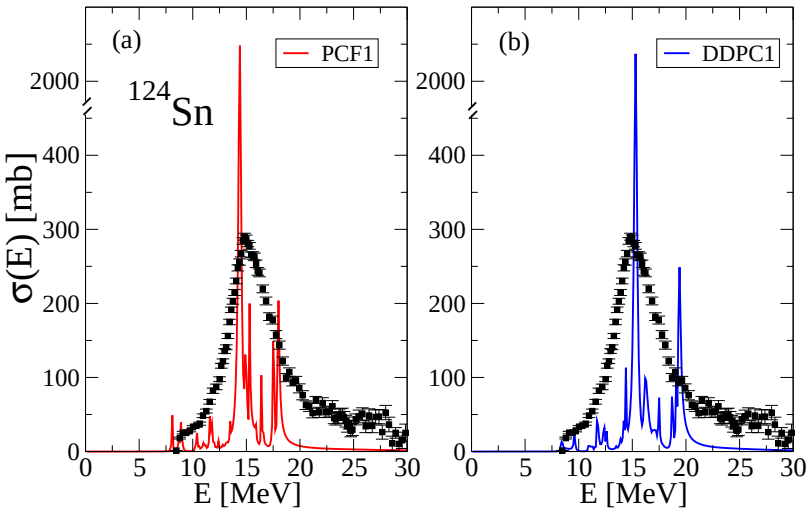

Figure 1. (Color online) The isovector dipole strength distribution in ^{124}Sn for the parameter set PC-F1 of Ref. [8] and the parameter set DD-PC1 of Ref. [9]. Relativistic continuum QRPA calculations [7] are compared with the experiment (black) of Ref. [10].

does not depend on energy. This approximation corresponds to the small amplitude limit of the time-dependent mean field equations, i.e. to RPA and QRPA and it is extensively used in nuclear physics [2]. As an example we show in Fig. 1 the distribution of the isovector dipole strength in the nucleus ^{124}Sn. In the relativistic case, so far, most of these applications have been done by diagonalizing the QRPA-matrix in a discrete basis. Here we compare recent relativistic continuum QRPA results [7] with the experimental dipole strength. As one can see, there is excellent agreement between the position of the peak of the resonance. However, it is clearly seen that the theoretical width is much smaller than the experimental value. This is typical for all heavy nuclei, where large Coulomb and centrifugal barriers prevent a coupling to the continuum. The large experimental width can only be explained by a coupling to more complicated configurations. In order to describe this coupling in a consistent microscopic way, we have to go back to Eq. 5 and take into account an energy dependence in the self-energy.

4. Energy dependence of the self energy $\Sigma(\omega)$.

In a relativistic many-body theory the motion of single nucleons in the nuclear medium is described by the Dyson equation

$$\big(\boldsymbol{\alpha}(\mathbf{p}-\boldsymbol{\Sigma})+\beta(m+\Sigma_s)+\Sigma_0\big)|\psi\rangle=\varepsilon|\psi\rangle. \tag{7}$$

where Σ_s and Σ_μ are the self energies. They correspond to the effective single particle $v[\rho](\mathbf{r},t)$ potential of time-dependent Kohn-Sham theory in Eq. 1. We decompose it in a stationary local part $\tilde{\Sigma}(\mathbf{r})$ and an energy-dependent non-local term

$$\Sigma(\mathbf{r},\mathbf{r}';\omega)=\tilde{\Sigma}(\mathbf{r})\delta(\mathbf{r}-\mathbf{r}')+\Sigma^e(\mathbf{r},\mathbf{r}';\omega), \tag{8}$$

where $\tilde{\Sigma}$ corresponds to the scalar and vector fields of the static RMF model. $\Sigma^e(\varepsilon)$ is derived from the particle-phonon coupling model [11]. From the solution of the Dyson equation one finds a fragmentation of the single-particle states and a corresponding reduction of the single-particle strength and an increasing level density at the Fermi surface.

For the description of giant resonances we use this self-energy and derive from it the effective interaction (3). We find two parts, the static interaction of the adiabatic approximation and an

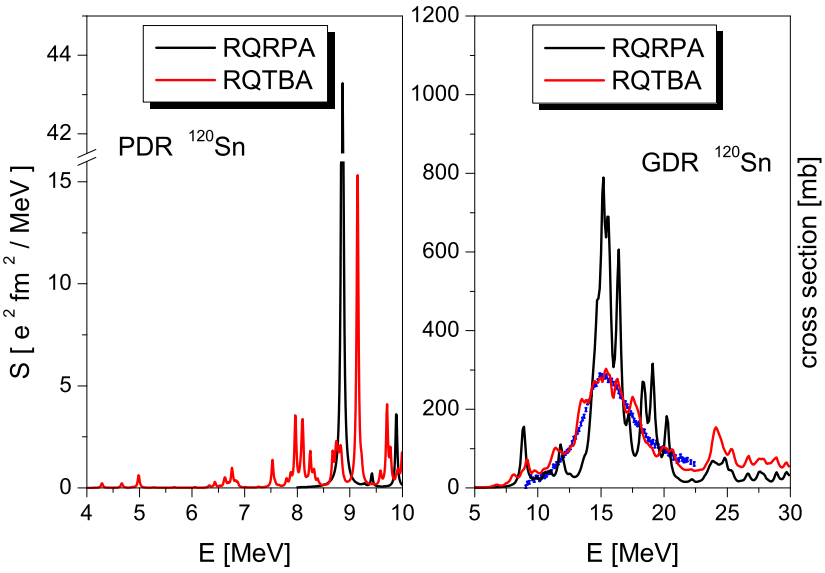

Figure 2. (Color online) The dipole spectra for ^{120}Sn calculated within RQRPA (black) and RQTBA (red) are compared with data (blue) of Ref. [15]. Right panel: photoabsorption cross sections computed with the artificial width 200 keV. Left panel: the low-lying portions of the corresponding spectra in terms of the strength function, calculated with 20 keV smearing.

induced energy dependent part $\Phi(\omega)$ (for a graphical representation see the first part of Fig. 3). As, on the one-body level, the energy dependence of the self energy $\Sigma^e(\omega)$ in the Dyson equation (7) leads to a fragmentation of the single particle spectrum by including $1p\otimes phonon$ (ie. $2p-1h$) configurations one finds now, on the two-body level, in the Bethe Salpeter equation because of the energy dependence of the induced interaction a strong fragmentation of the phonon spectrum by including $1p1h\otimes phonon$ (i.e. $2p-2h$) configurations. This causes the spreading width of giant resonances and a redistribution of the pygmy strength.

Two essential approximations are used in this context: (i) the *Time-Blocking Approximation* (TBA) introduced by Tselyaev in Ref. [12] and extended to relativistic systems (RTBA) and (RQTBA) in Refs. [13, 14], (ii) a *renormalization of the effective interaction*, by replacing $\Phi(\omega)$ by the difference $\Phi(\omega)-\Phi(0)$. This avoids double counting.

In Fig. 2 we show the dipole spectrum for the tin isotope ^{120}Sn. The right panel shows the photoabsorption cross section. The spectrum is dominated by the IVGDR. It is seen that the envelope of the calculated GDR in ^{120}Sn between 10 and 22 MeV, where data are available, is in excellent agreement to the experimental cross section. This is particularly satisfying since these results are obtained in a fully consistent way from the parameter set NL3 without any additional fit parameter. It indicates that the mechanism of coupling to the surface phonons provides the major contribution to the width of these resonances.

The left panel of Fig. 2 shows the low-lying parts of the E1 response in terms of the strength function. The black very sharply peaked curves correspond to RQRPA and the red fragmented curves to RQTBA calculations. Experimental data are taken from the EXFOR database [15]. These figures clearly demonstrate how the two-quasiparticle states, which are responsible for the spectrum of the RQRPA excitations, are fragmented through the coupling to the collective vibrational states. It is clearly seen how the low-lying strength develops with the increase of the neutron excess. It is found that the pygmy mode show a pronounced peak on the QRPA level, which is fragmented when the phonon coupling is switched on, but it is not washed out totally.

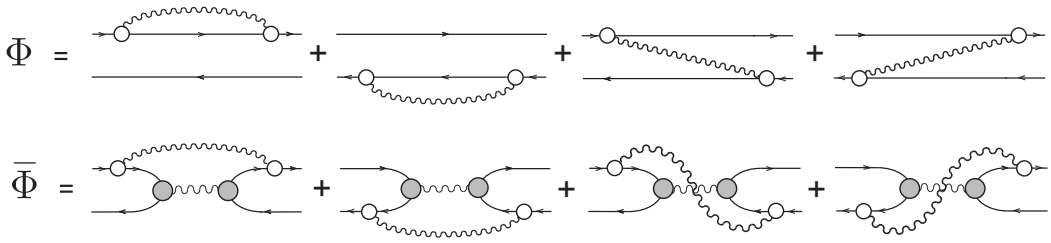

Figure 3. The 2q⊗phonon amplitude Φ of the conventional phonon coupling model and the two-phonon amplitude $\bar{\Phi}$ of the two-phonon model in a diagrammatic representation. The wavy curves denote phonon propagators, the empty circles represent phonon vertices, and the grey circles together with the two nucleonic lines denote RQRPA transition densities.

5. Coupling of two phonons

The main assumption of the relativistic quasiparticle time-blocking approximation (RQTBA) [14] discussed so far is that two types of elementary excitations – two-quasiparticle and vibrational modes – are coupled in such a way that configurations of $2qp \otimes phonon$ type with low-lying phonons strongly compete with simple $2qp$-configurations close in energy. There are however additional processes, which are not fully included in this scheme as for instance the coupling of two low-lying collective phonons, e.g. the first 2^+_1 and the first 3^-_1 state, to a phonon multiplet $[2^+_1 \otimes 3^-_1]$. Therefore, recently an extension of RQBTA has been introduced, which includes also the coupling to 2-phonon states [17].

In the diagrammatic representation of the amplitude $\Phi(\omega)$ in the upper line of the Fig. 3 the intermediate $1p1h$-propagator is represented by the two straight nucleonic lines between the circles denoting the amplitudes of emission and absorption of the phonon by a single particle (or hole). In RQTBA-2 one introduces the RQRPA correlations into the intermediate $1p1h$-particle propagator replacing the amplitude $\Phi(\omega)$ by the new one $\bar{\Phi}(\omega)$.

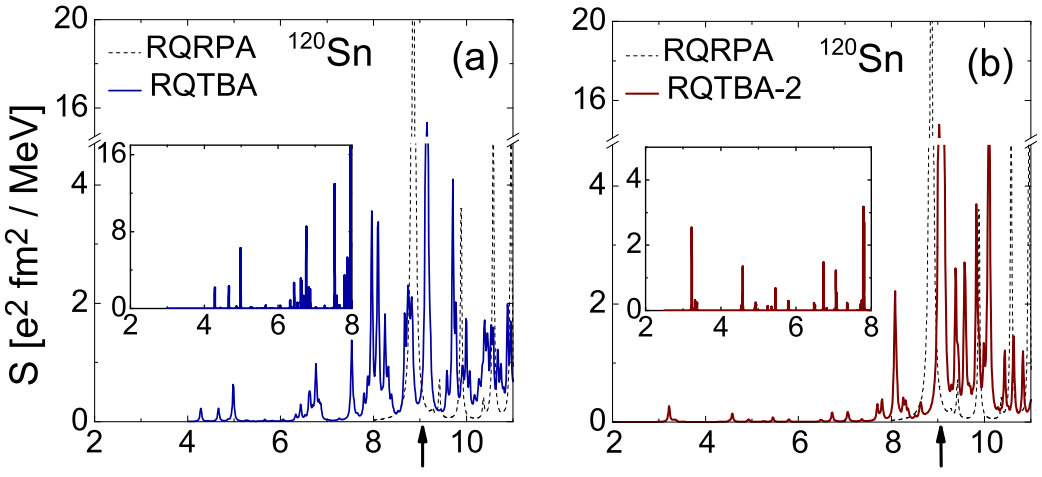

Figure 4. (Color online) Low-lying dipole spectrum of ^{120}Sn calculated within the RQRPA (dashed curves), RQTBA (blue solid curve, panel (a)) and RQTBA-2 (red solid curve, panel (b)). A finite smearing parameter $\Delta = 20$ keV has been used in the calculations. The insert shows the zoomed pictures of the spectra below 8 MeV with a small value $\Delta = 2$ keV allowing to see all the states in this energy region. The arrows indicate the experimental neutron threshold.

Fig. 4 illustrates the effect of two-phonon correlations on spectra of nuclear excitations. It displays the dipole strength function of ^{120}Sn calculated within the conventional RQTBA and the two-phonon RQTBA-2. The resulting strength functions are compared with the RQRPA strength function because both of them originate from the RQRPA by similar fragmentation mechanisms. Here the major fraction of the RQRPA pygmy mode shown by the dashed curve is pushed up above the neutron threshold by the RQTBA-2 correlations. A low lying 1^- state appears at 3.22 MeV with $B(E1)\uparrow = 14{\times}10^{-3}$ e^2 fm^2. These numbers can be compared with the corresponding data of Ref. [18] for the lowest 1^- state: it is observed at 3.28 MeV with a $B(E1)\uparrow = 7.60(51){\times}10^{-3}$ e^2 fm^2 in ^{120}Sn.

6. Summary and conclusions

Several recent applications of density functional theory for excited states have been discussed. In the adiabatic approximation, where the self-energy does not depend on energy, simple QRPA calculations in the continuum reproduce the position of giant resonance, but not the width. Energy dependent self-energies lead to induced energy-dependent interactions. On the $2qp$-phonon level we can reproduce the width successfully, but one has to go further to include also the coupling to 2-*phonon*-configurations properly. This can be done by including higher correlations in the kernel of the Bethe-Salpeter equation.

Of course there are open problems. Some of them are of technical nature: so far pairing is treated on a very primitive level with a seniority zero force in the BCS scheme and the continuum is only on the QRPA level properly taken into account. Others are more complicated to solve. Ground state correlations for instance are, so far, only taken into account on the RPA level. One could also think about further extensions of the TBA in order to include such effects also in the kernel of the Bethe Salpeter equation. At the moment these calculations are restricted to spherical nuclei. In deformed nuclei the numerical effort is considerably larger and in addition we have the problem of symmetry violation.

Acknowledgments

This work was supported by the FNRS (Belgium) and the Communauté française de Belgique,the Hessian LOEWE initiative through the Helmholtz International Center for FAIR, and by the excellence cluster "Origin and Structure of the Universe " (www.universe-cluster.de).

References

[1] Ring P 1996, *Prog. Part. Nucl. Phys.* **37** 193
[2] Vretenar D, Afanasjev A V, Lalazissis G A and Ring P 2005, *Phys. Rep.* **409** 101
[3] Kohn W and Sham L J 1965, *Phys. Rev.* **137**, A1697
[4] Marques M A L, Ullrich C A, Nogueira F, Rubio, Burke A, and Gross E K U (Eds.) 2006, *Time-Dependent Density Functional Theory* (Heidelberg: Springer-Verlag)
[5] Runge E and Gross E K U 1984, *Phys. Rev. Lett.* **52**, 997
[6] Ring P and Schuck P 1980, *The Nuclear Many-Body Problem* (New York: Springer-Verlag)
[7] Daoutidis I and Ring P 2011, *Phys. Rev.* **C83**, 044303
[8] Bürvenich T, Madland D G, Maruhn J A, and Reinhard P-G, 2002, *Phys. Rev.* **C65**, 044308
[9] Nikšić T, Vretenar D, and Ring P 2008, *Phys. Rev.* **C78** 034318
[10] Fultz S C, Berman B L, Caldwell J T, Bramblett R L, Kelly M A 1969, *Phys. Rev.* **186** 1255
[11] Litvinova E and Ring P 2006, *Phys. Rev.* **C73**, 044328
[12] Tselyaev V I 1989, *Sov. J. Nucl. Phys.* **50**, 780
[13] Litvinova E, Ring P, and Tselyaev V I 2007, *Phys. Rev.* **C75**, 064308
[14] Litvinova E, Ring P, and Tselyaev V I 2008, *Phys. Rev.* **C78**, 014312
[15] Experimental Nuclear Reaction Data, http://www-nds.iaea.or.at/exfor/exfor00.htm.
[16] Litvinova E, Ring P, and Vretenar D 2007, *Phys. Lett.* **B647**, 111
[17] Litvinova E, Ring P, and Tselyaev V I 2010, *Phys. Rev. Lett.* **105**, 022502
[18] Bryssinck J *et al*, 1999, *Phys. Rev.* **C59**, 1930